

1 Electronic Supplementary Information (ESI)
2 **Engineering a hierarchically micro-/nanostructured Si@Au-**
3 **based artificial enzyme with improved accessibility of active**
4 **sites for enhanced catalysis**

5

6 Jian Wang,^a Bo Ye,^b Shiqi Xiao,^b Xia Liu*^a

7

8 ^a School of Chemistry, Southwest Jiaotong University, Chengdu 610031, China.

9 ^b College of Life Science and Engineering, Southwest Jiaotong University, Chengdu
10 610031, China

11 *E-mail: xliu@swjtu.edu.cn.

12

13 **Additional Experimental Section**

14 **Additional Scheme 1**

15 **Additional Figures S1-S11**

16 **Additional Tables S1-S5**

17 **Additional References**

18

19 **1. Additional Experimental Section**

20 **1.1. Characterization**

21 The Ultraviolet-visible (UV-Vis) absorption spectra were recorded using a P4 UV-
22 Vis spectrophotometer. Fourier transform infrared (FTIR) spectroscopy was carried out
23 on a Bruker Tensor 27 FTIR spectrometer. A field emission scanning electron
24 microscope (SEM) (JSM 7800F Prime) was applied to determine the morphology of
25 as-prepared microspheres. The SEM samples were prepared by depositing a dilute
26 ethanol dispersion of the as-prepared microspheres onto the surface of a silicon wafer.
27 Transmission electron microscopy (TEM) (JEM-2100F) equipped with an energy-
28 dispersive X-ray spectrum was applied to determine the structural and chemical
29 characteristics of the as-prepared microspheres. TEM images and high-angle annular
30 dark-field scanning TEM (HAADF-STEM) were recorded using a JEM-2100F high-
31 resolution transmission electron microscope operating at 200 kV. The TEM samples
32 were prepared by dispersing synthesized products in ethanol by sonication and then
33 depositing onto a holey carbon film supported by copper grids. X-ray photoelectron
34 spectra (XPS) were collected on a Kratos Axis Ultra X-ray photoelectron spectrometer
35 (Thermo Scientific ESCALAB Xi+). The crystalline structures of the as-prepared
36 microspheres were evaluated by X-ray diffraction (XRD) analysis on an Ultima IV X-
37 ray diffractometer with Ni-filtered Cu K α radiation. The operation voltage and current
38 were kept at 40 kV and 40 mA. N₂ adsorption-desorption isotherms were recorded on
39 a Micromeritics 3Flex automated sorption analyzer. The pore size was determined
40 following the Barrett-Joyner-Halenda (BJH) method.

41 **1.2. Fabrication of smooth silica microspheres with low surface thiol density** 42 **using a post-grafting method**

43 Smooth silica microspheres (SSM) were prepared according to the previously
44 reported method with slight modifications.¹ Briefly, 12.8 mL of ethanol and 2.3 mL of
45 ammonium hydroxide (28%) were added sequentially to 5 mL of water. After stirring
46 for 30 min, 2.26 mL of tetraethyl orthosilicate was added dropwise over 1 min. The
47 reaction was stirred at room temperature for 24 h. The products were collected by

48 centrifugation at 5000 rpm for 3 min and washed three times with ethanol and deionized
49 water to remove the residual reaction products, respectively. The obtained pure solid
50 product was then put into a vacuum drying oven for 12 h at 37 °C to finally obtain 0.55
51 μm smooth silica microspheres.

52 The sample (20 mg) was dispersed in toluene (15 mL) under nitrogen. After stirring
53 for 1 h at 110 °C, a certain amount of MPTMS was added and the mixture was refluxed
54 for 18 h under nitrogen.² The product was centrifuged, washed with toluene and ethanol
55 three times, and then dried under vacuum at 50 °C. The sample prepared by the post-
56 grafting method was called smooth silica microspheres low surface thiol density (SSM-
57 L).

58 **1.3. Fabrication of smooth silica microspheres with high surface thiol density** 59 **using the one-pot synthesis without CTAB**

60 Smooth silica microspheres with high surface thiol density (SSM-H) were prepared
61 according to the previously reported method with slight modifications.³ Briefly, 0.25 g
62 of PVA is rapidly dissolved in 5 mL of water by sonication. Keeping the stirring speed
63 constant, 8 mL of methanol and 2 mL of ammonia (5.6%) were added sequentially to
64 the solution. After stirring for 15 min, a certain amount of MPTMS was added dropwise
65 over 15 s. The reaction was stirred at room temperature for 24 h. The products were
66 collected by centrifugation at 5000 rpm for 3 min and washed three times with ethanol
67 and deionized water to remove the residual reaction products, respectively. The
68 obtained pure solid product was then put into a vacuum drying oven for 12 h at 37 °C
69 to finally obtain smooth silica microspheres with high surface thiol density (SSM-H).

70 **1.4. Ellman's assay**

71 The Ellman reagent method is a typical technical method used to measure the surface
72 density of sulfhydryl groups.⁴ In a typical procedure, DTNB²⁻ solution was made by
73 dissolving sodium acetate (41 mg) and DTNB²⁻ (7.96 mg) in water (10 mL). To prepare
74 the blank sample, DTNB²⁻ solution (100 μL) was added to Tris buffer solution (200 μL ,
75 1 M, pH 8) and then diluted in water (1700 μL). The nanoparticle solution (20 μL , 2.5
76 mg mL^{-1}) and DTNB²⁻ solution (100 μL) were added to Tris buffer solution (200 μL , 1
77 M, pH 8) and then diluted in water (1680 μL), mixed carefully using a pipette, and then

78 incubated at room temperature for 5 min. The mixture was centrifuged and the
79 absorbance of the supernatant was measured at 412 nm. The quantity of the surface
80 thiol groups was calculated by dividing absorbance by the extinction coefficient of the
81 reagent ($13600 \text{ M}^{-1}\text{cm}^{-1}$).

82 **1.5. Peroxidase activity assessment of Au-containing system**

83 To study the peroxidase like study of Au-containing system for TMB oxidation, we
84 used a total of 2 mL solution and all the absorption measurements were carried out
85 using P4 UV-Visible spectrophotometry. In a 5 ml centrifuge tube, we separately added
86 (1 mL) aqueous solution of Au-containing system (SoS-0.55, SSM-L@Au-7.8, SSM-
87 H@Au-7.6 and SoS-0.55@Au-7.3). (500 μL) H_2O_2 and (500 μL) TMB were added to
88 the centrifuge tube and react for 2 minutes. Afterwards, the reaction solution was
89 centrifuged for 1 minute and the reaction solution was aspirated for UV spectroscopy.
90 Control samples were made by replacing the Au-containing system with DI water.

91 **1.6. Peroxidase activity assessment of SoS-0.55@Au-s**

92 The peroxidase-like activity of the synthesized SoS-0.55@Au-s was measured based
93 on the steady-state kinetic study. The catalytic ability of SoS-0.55@Au-s was measured
94 by P4 UV-Visible spectrophotometry. All assays were carried out at room temperature
95 in quartz cuvettes [path length (l) = 1.0 cm] using sodium acetate buffer (100 mM, pH
96 4) as the reaction buffer. The absorbance of the produced blue color at 652 nm
97 represents the released TMB diimine product.⁵ In a typical experiment, SoS-0.55@Au-s
98 (400 μg) was dispersed in sodium phosphate (1000 μL) and then placed in the cuvette.
99 H_2O_2 (500 μL) and TMB (500 μL) were added to the cuvette and the increase of
100 absorbance at 652 nm was immediately measured as a function of time (5 s intervals)
101 for 2 min. The relative activity was defined as the absorbance of SoS-0.55@Au-s to
102 that of SoS-0.55-@Au-7.3.

103 **1.7. Estimation of kinetic parameters**

104 To measure the kinetic parameters for SoS-0.55@Au-7.3, kinetic assays were
105 conducted using SoS-0.55-@Au-7.3 (40 μg) dispersed in sodium phosphate (200 μL)
106 and H_2O_2 (final concentration of 50 mM) as the reaction media at 35 °C. Various
107 concentrations of TMB were added to the cuvette and the absorbance at 652 nm was

108 instantly measured as a function of time with intervals of 5 s for 2 min. The obtained
109 “absorbance versus time” plots were then used to calculate the slope at the initial point
110 ($\text{slope}_{\text{initial}}$) of each reaction. The initial reaction velocity (v) was calculated by dividing
111 $\text{slope}_{\text{initial}}$ by $(\epsilon_{\text{TMB-652nm}} \times l)$, where $\epsilon_{\text{TMB-652nm}}$ represents the molar extinction
112 coefficient of TMB at 652 nm which equals to $3.9 \times 10^4 \text{ M}^{-1} \text{ cm}^{-1}$.⁶

113 Nonlinear regression of the Michaelis-Menten equation [$v = V_{\text{max}} \times [S] / (K_{\text{m}} + [S])$]
114 was used to fit the plots of v against TMB concentrations ($[S]$). Lineweaver-Burk plot
115 was created from the Michaelis Menten equation to obtain the kinetic parameters, K_{m}
116 and V_{max} . V_{max} and K_{m} are the highest reaction rate and the Michaelis constant,
117 respectively.⁷

118 **1.8. Reusability assay**

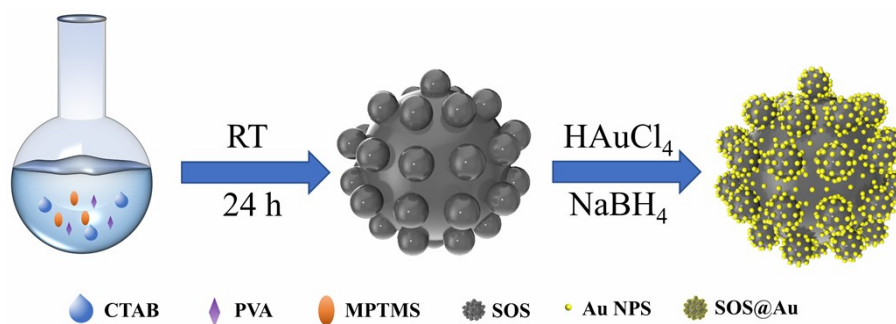
119 The reusability of SoS-0.55@Au-7.3 was studied by repeating the use of artificial
120 enzymes to catalyze the oxidation reaction of TMB. After each cycle (2 min), the
121 absorbance was read and the artificial enzymes were then separated from the reaction
122 system by centrifugation, washed three times with buffer solution to remove all of the
123 substrate and products from the samples, and applied in the next activity measurement
124 with fresh substrates. The relative activity was defined as the observed absorbance of
125 each cycle to the absorbance of the first cycle.

126 **1.9. H₂O₂ detection assay**

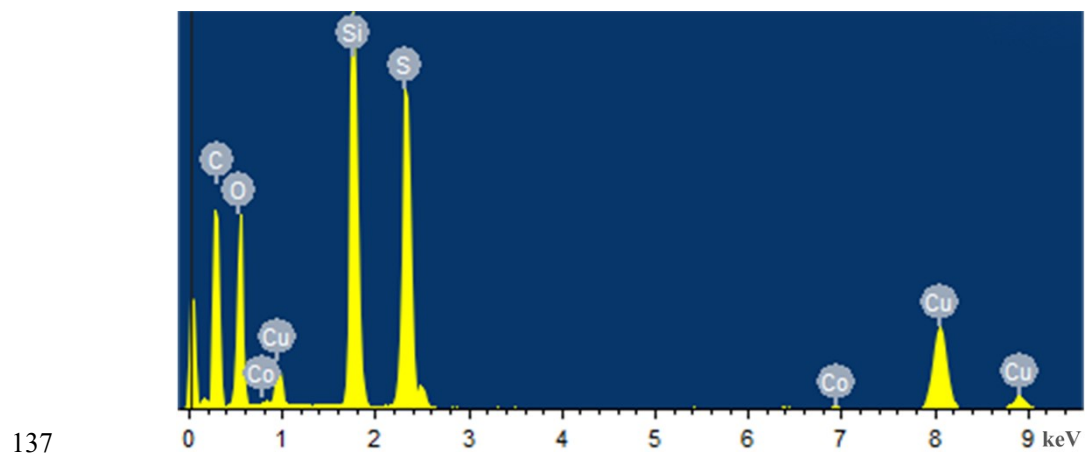
127 Various concentrations of H₂O₂ in sodium acetate buffer (100 mM, pH 3) were
128 reacted with 200 $\mu\text{g mL}^{-1}$ SoS-0.55@Au-7.3 and 1 mM TMB in a total volume of 200
129 μL . After incubated at 40 °C for 15 min, the reaction mixture was treated as the previous
130 description.

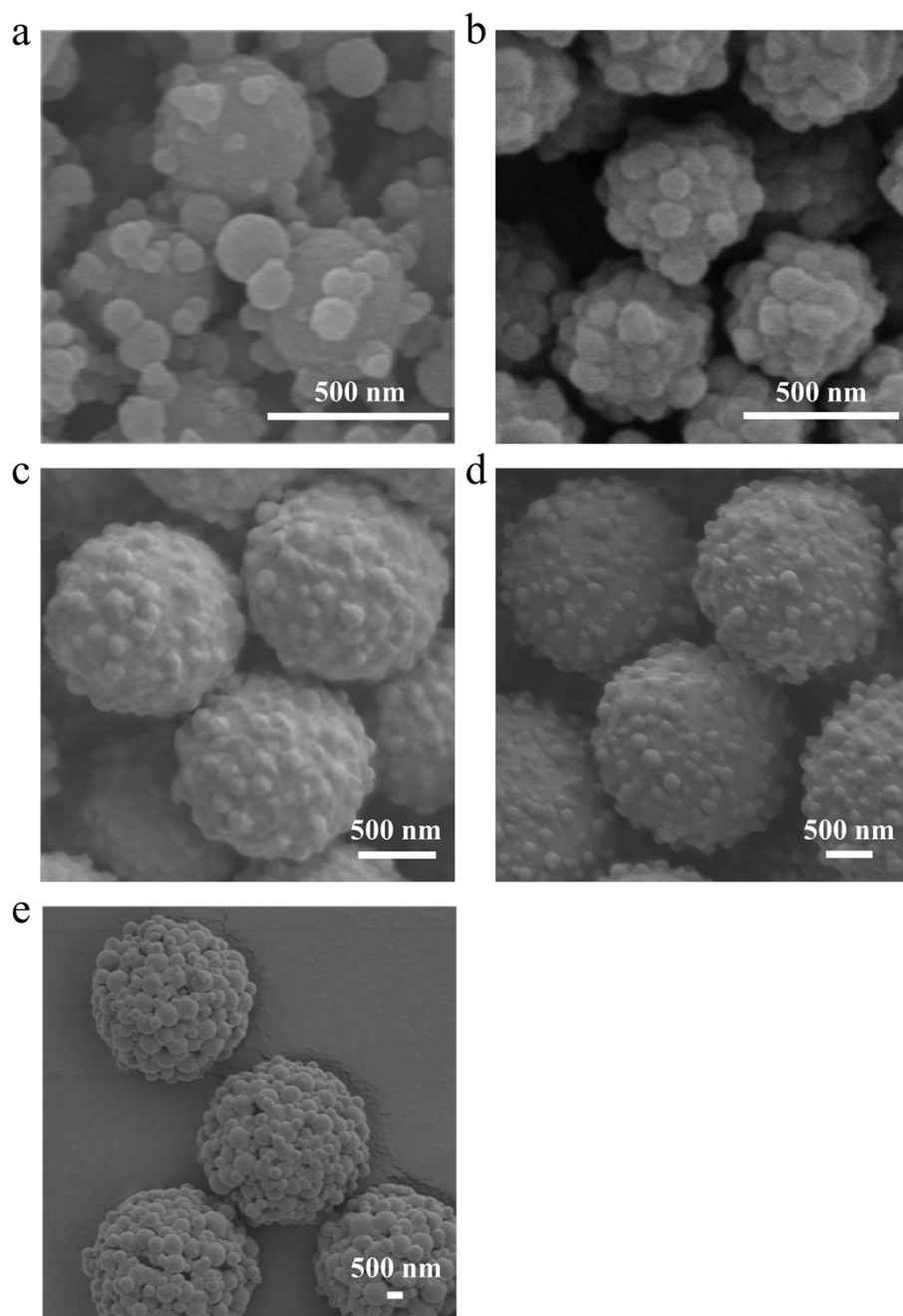
131

132 **2. Additional Scheme**



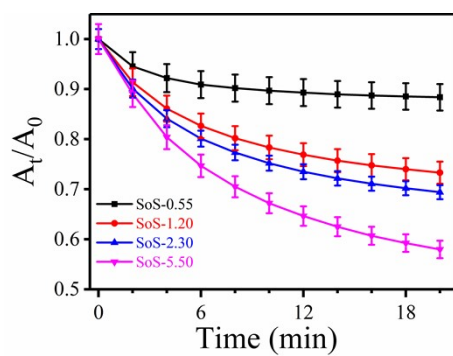
136 **3. Additional Figures**





140

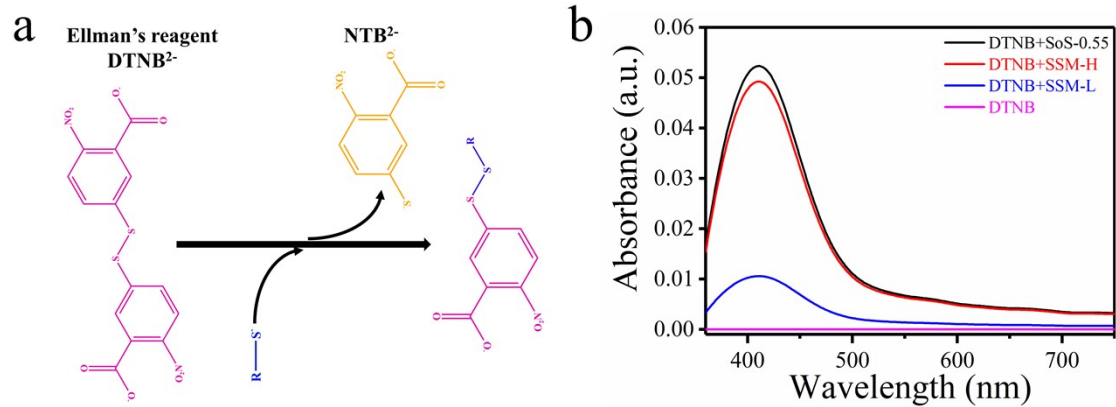
141 **Fig. S2** The effect of the MPTMS concentration on the size and morphology of SoS
142 silica microspheres: the SEM images of the SOS silica microspheres prepared using 9.1
143 mM MPTMS (a), 12.6 mM MPTMS (b), 36.1 mM MPTMS (c), 72.2 mM MPTMS (d),
144 and 180.5 mM MPTMS (e).



145

146 **Fig. S3** The relative absorbance (A_t/A_0) of SoS-X ($X = 0.55, 1.20, 2.30, \text{ and } 5.50 \mu\text{m}$)
147 silica microspheres dispersed in water as a function of settling time, where A_0 and A_t
148 represent the absorption values of the microsphere solution after settling for 0 and t
149 min.

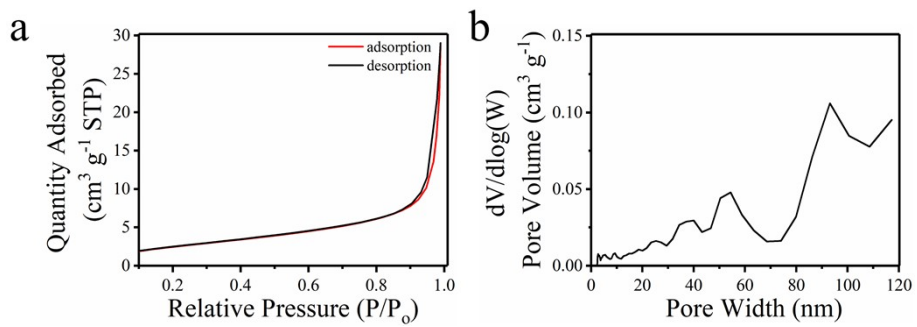
150



151

152 **Fig. S4** (a) Schematic diagram of the Elman test method for the determination of thiol
 153 groups and (b) the absorbance spectra of the reaction product NTB²⁻ of DTNB²⁻ in
 154 different reaction systems.

155

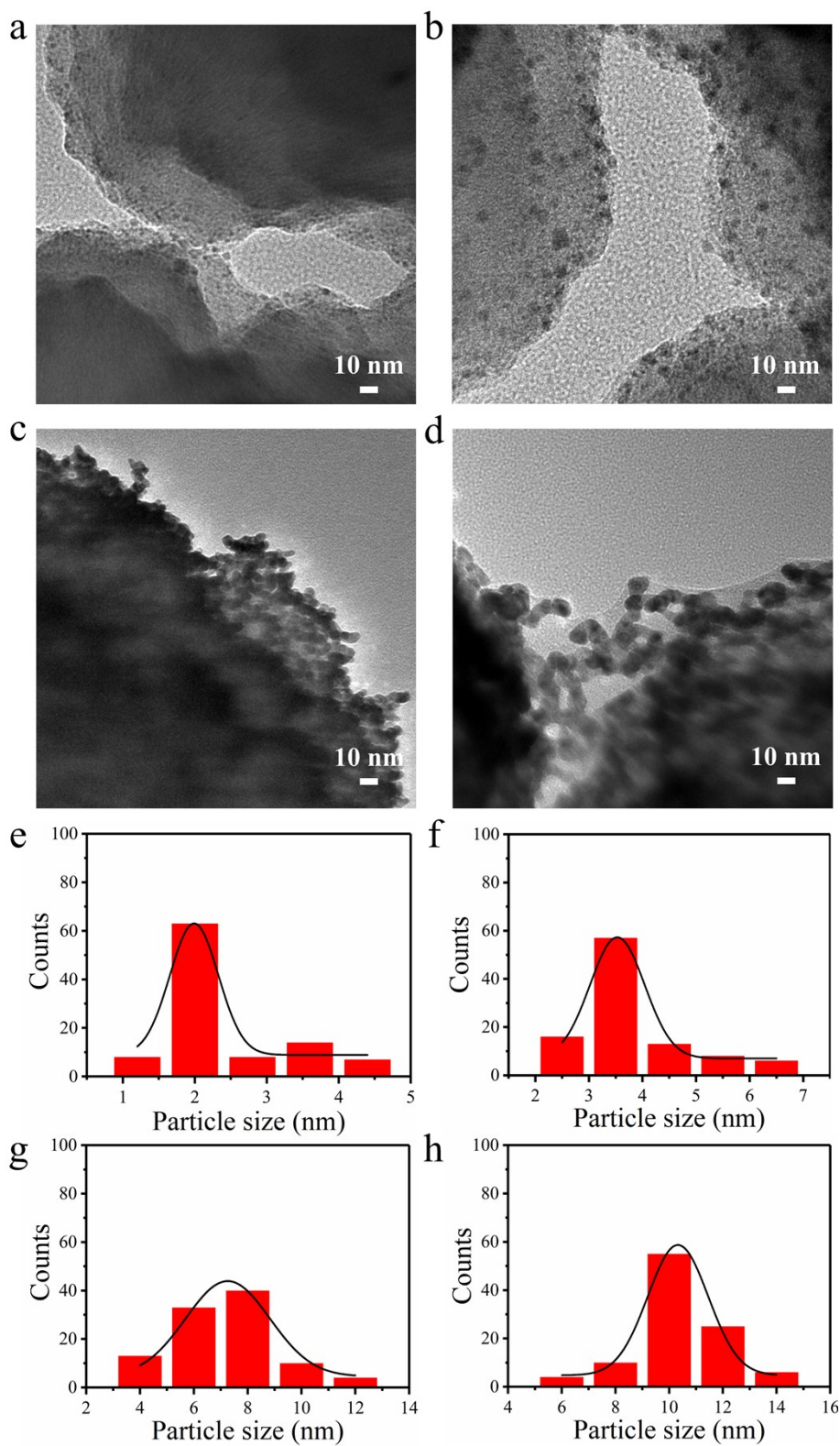


156

157 **Fig. S5** (a) N₂ sorption isotherms and (b) the pore size distribution curve of SoS-0.55

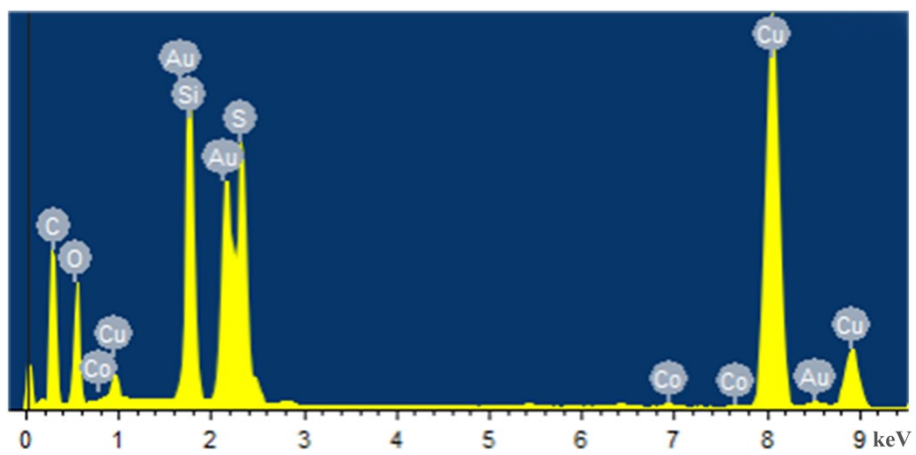
158 silica microspheres.

159



160

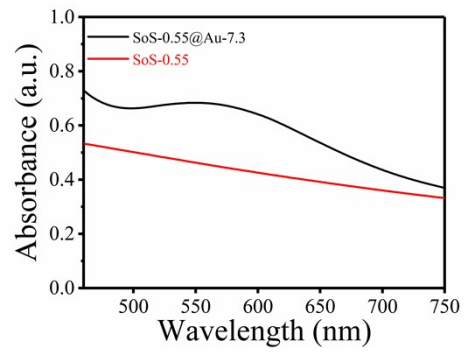
161 **Fig. S6** (a-d) Selected high-magnification TEM images of SoS-0.55@Au-s ($s = 2.1$,
 162 3.5, 7.3 and 10.3 nm), the scale bar is 10 nm. (e-h) The size distribution histogram of
 163 SoS-0.55@Au-s, the total number of AuNPs counted for the histogram was 100.



164

165 **Fig. S7** The EDS spectra of SoS-0.55@Au-7.3.

166

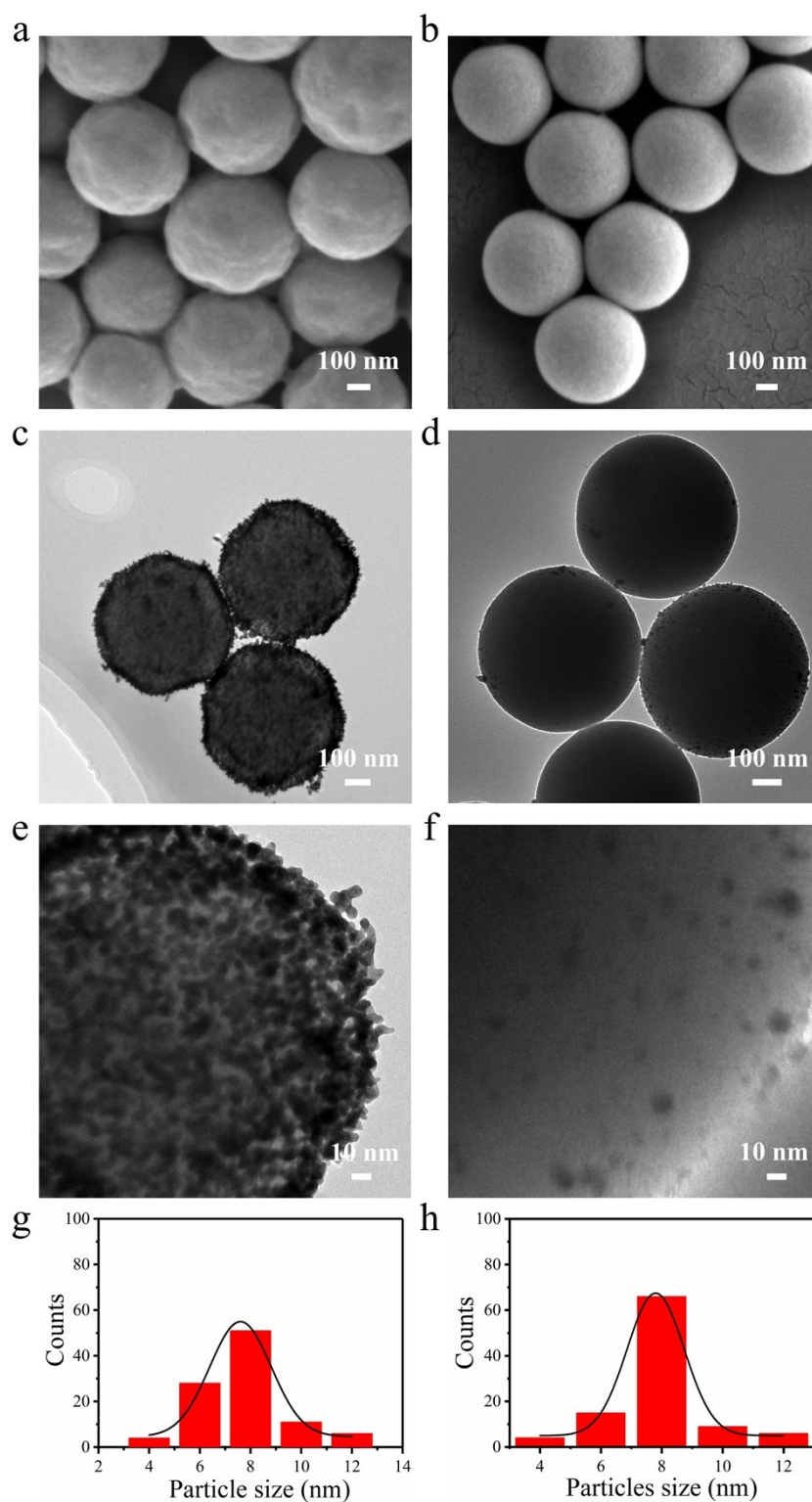


167

168 **Fig. S8** UV-Vis absorption spectra of SoS-0.55@Au-7.3 (black curve) and SoS-0.55

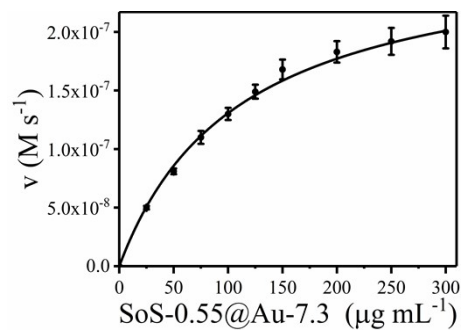
169 silica microspheres (red curve).

170



171

172 **Fig. S9** SEM images of SSM-H (a) and SSM-L (b). TEM images of SSM-H@Au-7.6
 173 (c) and SSM-L@Au-7.8 (d). High-resolution TEM images of SSM-H@Au-7.6 (e) and
 174 SSM-L@Au-7.8 (f). The size distribution histogram of SSM-H@Au-7.6 (g) and SSM-
 175 L@Au-7.8 (h). The total number of AuNPs counted for the histogram was 100.



176

177 **Fig. S10** The rates of TMB oxidation by H_2O_2 using variable concentrations of SoS-

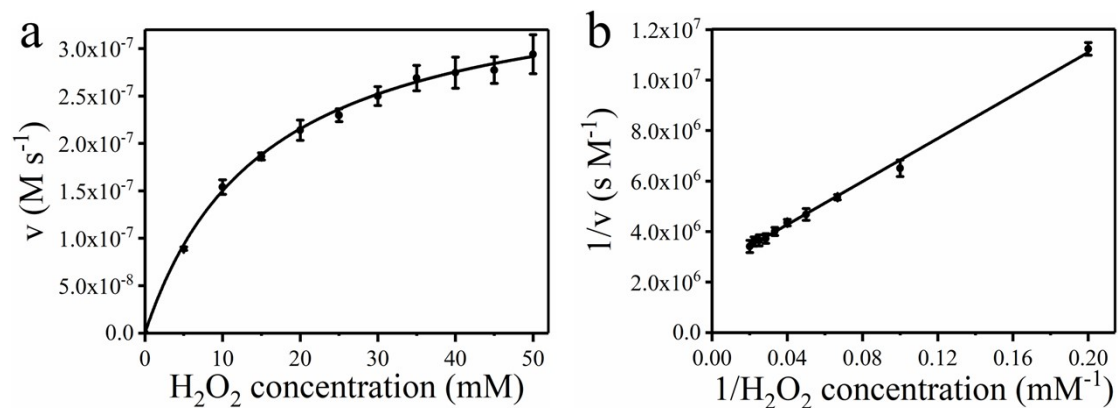
178 0.55@Au-7.3 in the presence of 0.5 mM TMB and 50 mM H_2O_2 : 0, 25, 50, 75, 100,

179 125, 150, 200, 250, 300 $\mu\text{g mL}^{-1}$, the total volume of the reaction mixture: 2 mL. All

180 the experiments were conducted in sodium acetate buffer (100 mM, pH 4).

181

182



183

184 **Fig. S11** (a) Steady-state kinetic assay of SoS-0.55@Au-7.3. Experiments were
185 performed in 0.1 M sodium acetate buffer (pH 4) with $200 \mu\text{g mL}^{-1}$ SoS-0.55@Au-7.3,
186 0.05 mM TMB and varied concentrations of H_2O_2 at 35 °C. (b) Lineweaver-Burk plot
187 of the inverse of the initial rate vs. the inverse of the substrate concentration for
188 estimating the kinetic parameters (K_m and V_{max}) of SoS-0.55@Au-7.3 using H_2O_2 as
189 the substrate.

191 **4. Additional Tables**192 **Table S1.** Detailed synthesis parameters for SoS-X silica microspheres and SSM-H.

Samples	MPTMS	PVA	CTAB	5.6% NH ₃ ·H ₂ O	Size
SoS-0.50	9.1 mM	0.25 g	0.2 g	2 mL	0.50 μm
SoS-0.55	12.6 mM	0.25 g	0.2 g	2 mL	0.55 μm
SoS-1.20	36.1 mM	0.25 g	0.2 g	2 mL	1.20 μm
SoS-2.30	72.2 mM	0.25 g	0.2 g	2 mL	2.30 μm
SoS-5.50	180.5 mM	0.25 g	0.2 g	2 mL	5.50 μm
SSM-H	12.6 mM	0.25 g	0 g	2 mL	0.55 μm

193

194

195 **Table S2.** Partial elemental content of SoS-0.55@Au-s (s = 2.0, 3.5, 7.3 and 10.3 nm),
196 SSM-H@Au-7.6 and SSM-L@Au-7.8.

Samples	Si	S	Au
SoS-0.55@Au-2.0	11.08 wt %	5.82 wt %	1.97 wt %
SoS-0.55@Au-3.5	10.48 wt %	6.23 wt %	8.06 wt %
SoS-0.55@Au-7.3	11.38 wt %	6.44 wt %	14.50 wt %
SoS-0.55@Au-10.3	10.91 wt %	6.83 wt %	20.47 wt %
SSM-H@Au-7.6	11.26 wt %	6.15 wt %	11.28 wt %
SSM-L@Au-7.8	25.19 wt %	1.22 wt %	2.61 wt %

197

198

199 **Table S3.** Detailed synthesis parameters for SoS-0.55@Au-s (s = 2.0, 3.5, 7.3 and 10.3
200 nm), SSM-H@Au-7.6 and SSM-L@Au-7.8.

No.	Samples	Dispersing solvent (DI water)	HAuCl ₄ (100 mM)	NaBH ₄ (100 mM)
1	SoS-0.55@Au-2.1	14.4 mL	0.1 mL	0.5 mL
2	SoS-0.55@Au-3.5	13.2 mL	0.3 mL	1.5 mL
3	SoS-0.55@Au-7.3	12.0 mL	0.5 mL	2.5 mL
4	SoS-0.55@Au-10.3	10.8 mL	0.7 mL	3.5 mL
5	SSM-H@Au-7.6	12.0 mL	0.5 mL	2.5 mL
6	SSM-L@Au-7.8	12.0 mL	0.5 mL	2.5 mL

201
202

203 **Table S4.** Comparison of kinetic parameters of HRP and various materials.

Nanozyme	K_m (mM)	V_{max} ($M s^{-1}$)	Ref.
HRP ⁶	0.041	4.3×10^{-8}	<i>ACS Nano</i> 2012 , 6, 3142-3151.
Ferromagnetic nanoparticles ⁸	0.098	3.44×10^{-8}	<i>Nat. Nanotechnol.</i> 2007 , 2, 577-583.
Graphene oxide ⁹	0.024	3.45×10^{-8}	<i>Adv. Mater.</i> 2010 , 22, 2206-2210.
Cobalt nanoflakes ¹⁰	2.020	4.74×10^{-8}	<i>Anal Bioanal Chem</i> 2017 , 409, 4225-4232.
C-Dot ¹¹	0.039	3.61×10^{-8}	<i>Chem. Commun.</i> 2011 , 47, 6695-6697.
Mesoporous silica-supported gold nanoparticles ⁵	0.041	12.7×10^{-8}	<i>Adv. Mater.</i> 2015 , 27, 1097-1104.
Dendritic fibrous nano-silica supported gold nanoparticles ¹²	0.220	17.1×10^{-8}	<i>J. Mater. Chem. B</i> 2018 , 6, 1600-1604.
T-DMSNs@Au ¹³	0.0407	25.9×10^{-8}	<i>ACS Appl. Mater. Interfaces</i> 2019 , 11, 13264-13272.
SoS-0.55@Au-7.3	0.033	34.6×10^{-8}	This work

206 **Table S5.** Comparison of different materials for H₂O₂ detection.

Nanozyme	Reaction substrate	Detection limit of H ₂ O ₂ (μM)	Ref.
α-AgVO ₃ microrods ¹⁴	TMB	2.0	<i>Microchim. Acta</i> 2017 , 185, 1-8.
Co ₃ (PO ₄) ₂ •8 H ₂ O ¹⁵	TMB	4.4	<i>Colloids Surf., A</i> 2022 , 647, 129031-129038.
CeO ₂ /NT-TiO ₂ @0.1 ¹⁶	TMB	3.2	<i>ACS Appl. Mater. Interfaces</i> 2015 , 7, 6451-6461.
N-doped TiO ₂ ¹⁷	TMB	2.5	<i>J. Colloid Interface Sci.</i> 2017 , 505, 1147-1157.
GO-PtNi ¹⁸	TMB	5.0	<i>Mater. Today Chem.</i> 2018 , 7, 35-39.
SoS-0.55@Au-7.3	TMB	1.6	This work

207

208

209 **5. Additional References**

- 210 1 W. Stöber, A. Fink and E. Bohn, *J. Colloid Interface Sci.*, 1968, **26**, 62-69.
- 211 2 R. L. Oliveira, W. He, R. J. M. Klein Gebbink and K. P. de Jong, *Catal. Sci.*
212 *Technol.*, 2015, **5**, 1919-1928.
- 213 3 A. Ahmed, H. Ritchie, P. Myers and H. Zhang, *Adv. Mater.*, 2012, **24**, 6042-
214 6048.
- 215 4 X. D. Wang, K. S. Rabe, I. Ahmed and C. M. Niemeyer, *Adv. Mater.*, 2015, **27**,
216 7945-7950.
- 217 5 Y. Tao, E. Ju, J. Ren and X. Qu, *Adv. Mater.*, 2015, **27**, 1097-1104.
- 218 6 M. Liu, H. Zhao, S. Chen, H. Yu and X. Quan, *ACS Nano*, 2012, **6**, 3142-3151.
- 219 7 Z. Chen, C. Zhao, E. Ju, H. Ji, J. Ren, B. P. Binks and X. Qu, *Adv. Mater.*, 2016,
220 **28**, 1682-1688.
- 221 8 L. Gao, J. Zhuang, L. Nie, J. Zhang, Y. Zhang, N. Gu, T. Wang, J. Feng, D.
222 Yang, S. Perrett and X. Yan, *Nat. Nanotechnol.*, 2007, **2**, 577-583.
- 223 9 Y. Song, K. Qu, C. Zhao, J. Ren and X. Qu, *Adv. Mater.*, 2010, **22**, 2206-2210.
- 224 10 Y. M. Wang, J. W. Liu, J. H. Jiang and W. Zhong, *Anal. Bioanal. Chem.*, 2017,
225 **409**, 4225-4232.
- 226 11 W. Shi, Q. Wang, Y. Long, Z. Cheng, S. Chen, H. Zheng and Y. Huang, *Chem.*
227 *Commun.*, 2011, **47**, 6695-6697.
- 228 12 R. Singh, R. Belgamwar, M. Dhiman and V. Polshettiwar, *J. Mater. Chem. B*,
229 2018, **6**, 1600-1604.
- 230 13 M. Kalantari, T. Ghosh, Y. Liu, J. Zhang, J. Zou, C. Lei and C. Yu, *ACS Appl.*
231 *Mater. Interfaces*, 2019, **11**, 13264-13272.
- 232 14 Y. Wang, D. Zhang and J. Wang, *Microchim. Acta*, 2017, **185**, 1-8.
- 233 15 L. J. Peng, H. Y. Zhou, C. Y. Zhang and F. Q. Yang, *Colloids Surf., A*, 2022,
234 **647**, 129031-129038.
- 235 16 H. Zhao, Y. Dong, P. Jiang, G. Wang and J. Zhang, *ACS Appl. Mater.*
236 *Interfaces*, 2015, **7**, 6451-6461.

- 237 17 M. Nasir, S. Rauf, N. Muhammad, M. Hasnain Nawaz, A. Anwar Chaudhry,
238 M. Hamza Malik, S. Ahmad Shahid and A. Hayat, *J. Colloid Interface Sci.*,
239 2017, **505**, 1147-1157.
- 240 18 T. Niu, X. Deng, R. Wang and C. Zhou, *Mater. Today Chem.*, 2018, **7**, 35-39.